Baseline LIGO-II implementation design description of the stiff active seismic isolation system

J. Giaime, B. Lantz, S. Richman, D. Debra, C. Hardham, J. How,

and W. Hua, for the stiff active seismic isolation team in the LSC.

1   Introduction

The seismic isolation needed for LIGO-II will require a dramatic technological change from the passive systems used in the initial LIGO detector. To take advantage of the improved thermal noise of a 30 kg test mass made of high-Q material and suspended with fused silica fibers, one must attenuate the ground motion by more than 10 orders of magnitude at 10 Hz. Active isolation of ground motion to reduce the root-mean-squared ground displacement and the displacement noise in the gravitational wave band, coupled with multiple pendulum suspensions, can make this possible. We describe here the mechanical features and active control design for such a system. For further details, please see:

`http://lsuligo.phys.lsu.edu/active/active.html`

While other approaches can be used to achieve this level of seismic isolation, the mechanically-stiff suspension in the active seismic isolation scheme described here has a number desirable features not otherwise easily obtained:

- The same compact core design can be used in both HAM and BSC LIGO vacuum tanks, with only mechanical interfacing specialized for the tank geometry.

- The stiff support of the optics table mounting surface will allow easy installation of the optics payload.

- Conventional wires and ribbon cables can be used to carry signals.

- The compact size of this system allows (in the BSC) longer suspensions to be used later if this should become necessary. This design preserves space for unanticipated elements in the existing LIGO chambers.

- Full active instrumentation allows dynamically-selectable operating modes, and continuous state monitoring.

1

Our design uses one stage external to the vacuum system and two stages inside the vacuum. These stages are mechanically connected with fairly **stiff** springs, with typical passive resonances in the 2-4 Hz range. **Active isolation using feedback:** For the inner stages, we then measure motion in all 6 degrees of freedom (DOF) for each stage, filter those signals, and feed them back to non-contacting force actuators between the stages, reducing the noise by a factor of the servo loop gain. **Active isolation using feedforward:** For the outside stage, we reduce noise by measuring the floor motion, and feeding the negative of this signal forward, filtered by the modeled mechanical transmission, floor-to-stage, thus cancelling most of the transmitted noise. The cancellation, here largely confined to lower frequencies, is limited only by our knowledge of the system's transmission properties.
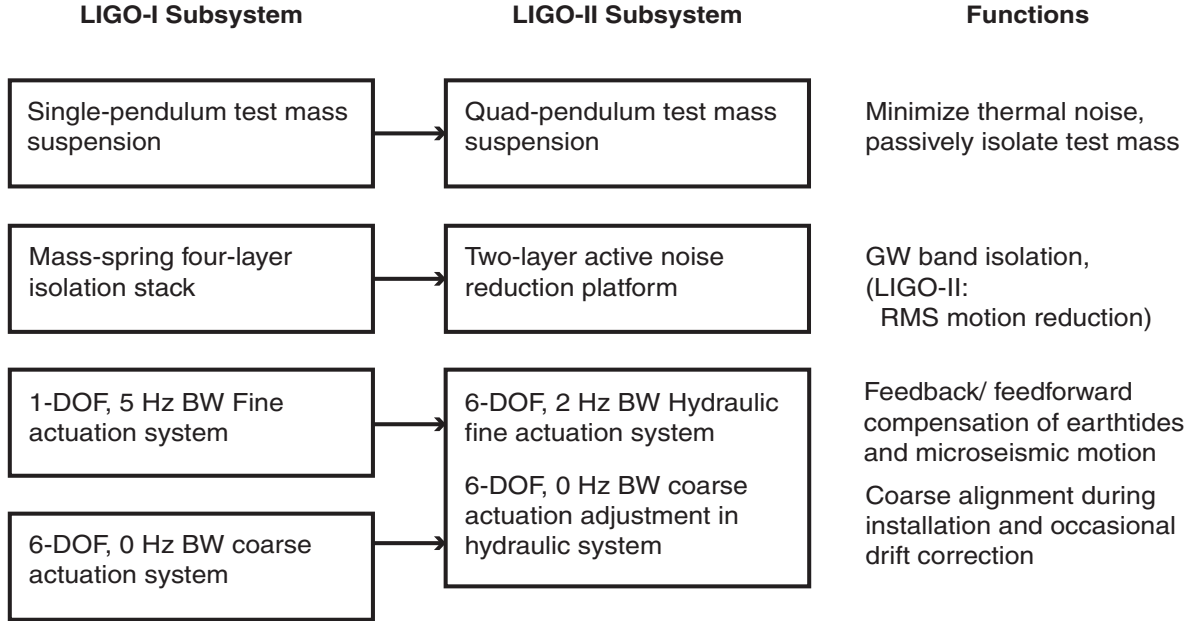
1.1   Motion requirements

LIGO-II's test mass suspension system is being developed by the GEO group at the University of Glasgow[5]. The interface between it and SEI as well as the performance requirements on SEI are set out in [1]. A well-defined interface has been chosen in order to allow independent testing of the two detector subsystems, and to facilitate their separate parallel development on different continents.

The BSC geometry requires SEI to support its payload from above (Figure 2) and the HAM geometry requires payload support from below (Fig. 3). This will require two different versions of our SEI design. However, a reference design has been chosen that limits the BSC/HAM differences to the interface and stage structures; the sensing, actuation, and control instrumentation that carries out the active isolation is identical in the two versions. In addition, the motion sensing and actuation is almost completely confined to "pods," which are field removable for service and replacement without disturbing the optics. These pods are also identical in the BSC and HAM designs. We expect that the performance and the implementation challenges of the two systems will be similar, so we will not generally differentiate between the two versions when describing the technology in this document.

It was not widely appreciated until recently that the displacement noise requirement on the HAM SEI, which must fit into fairly tight quarters, is more stringent than that for the BSC. At 10 Hz the BSC test mass suspension in LIGO-II will transmit only 2×10^{-8} of the vibration present at its suspension point at 10 Hz [5]; the shorter suspension for the HAM transmits 1×10^{-5}. The required 10 Hz test mass noise is 1×10^{-19} m/$\sqrt{\text{Hz}}$ for the sensitive optics in the BSC and 3×10^{-18} m/$\sqrt{\text{Hz}}$ for the HAM suspensions that support the mode cleaner mirrors [1]. So, we require a displacement noise level of 5×10^{-12} m/$\sqrt{\text{Hz}}$ on the BSC suspension mounting table and 3×10^{-13} m/$\sqrt{\text{Hz}}$ on the HAM table. We assume that motion in the (transverse) vertical direction can add to this noise with a factor of 1/1000, and since the current estimates from Glasgow[5] indicate vertical pendulum transmission not more than 1000 times as much as that in the horizontal, these requirements are unaffected as long as the suspension point is equally quiet in all directions.

There is another important set of requirements on the test mass motion, the root-mean-squared (RMS) displacement, velocity and angles. These requirements are intended to be met during operation of the global length and angle (ISC) control servos. Since the LIGO community has not yet designed the ISC subsystem, we are forced to make reasonable assumptions about its eventual design to apply the test mass motion requirements to SEI

LIGO-I Subsystem	LIGO-II Subsystem	Functions
Single-pendulum test mass suspension	Quad-pendulum test mass suspension	Minimize thermal noise, passively isolate test mass
Mass-spring four-layer isolation stack	Two-layer active noise reduction platform	GW band isolation, (LIGO-II: RMS motion reduction)
1-DOF, 5 Hz BW Fine actuation system	6-DOF, 2 Hz BW Hydraulic fine actuation system	Feedback/ feedforward compensation of earthtides and microseismic motion
6-DOF, 0 Hz BW coarse actuation system	6-DOF, 0 Hz BW coarse actuation adjustment in hydraulic system	Coarse alignment during installation and occasional drift correction

Figure 1: Seismic isolation functions in LIGO-I and LIGO-II, broken down by subsystem. Note that the present fine and coarse actuators are replaced by a hydraulic system in this design, and that an additional function, RMS motion reduction, is now required. The pendulum suspension, though not part of SEI, is shown because it contributes significant seismic isolation.

performance. Ken Strain and the GEO suspension group have provided a matlab program that allows the user to calculate the RMS motion based on global feedback to the SUS elements. Our RMS estimates for the longitudinal degrees of freedom are based on values obtained with this code. The displacement (velocity) requirements in the beam direction are 1×10^{-14} m (1×10^{-9} m/s) for BSC-based optics and 1×10^{-13} m (1×10^{-8} m/s) for HAM-based optics. Without *any* noise reduction in SEI, reference [5] shows that the BSC requirement can be met with global feedback to the elements of the SUS, albeit with a 200 Hz upper unity gain frequency. The noise reduction that SEI contributes allows the SUS controllers to have significantly less control authority and/or bandwidth. The RMS angle requirements stated in [1] are 1×10^{-9} radian, and we expect that any active system that meets the displacement requrement can meet this requirement, as long as sufficent gain is designed into the angle control loops, roughly as much as is used in LIGO-I (2 Hz upper unity gain frequency.)

1.2   Functional breakdown

Our overall design consists of a hydraulic actuator outside the vacuum chamber and a two-stage active seismic isolation platform inside the chamber. Figure 1 shows the roles of the various parts of the SEI and SUS in LIGO-I and LIGO-II.

The present external fine actuators are used in LIGO-I to translate, only in the beam direction, the in-vacuum SEI systems by ± 90 μm with an actuation bandwidth of several hertz. LIGO-I also has coarse actuators that can move ± 5 mm. These systems will be
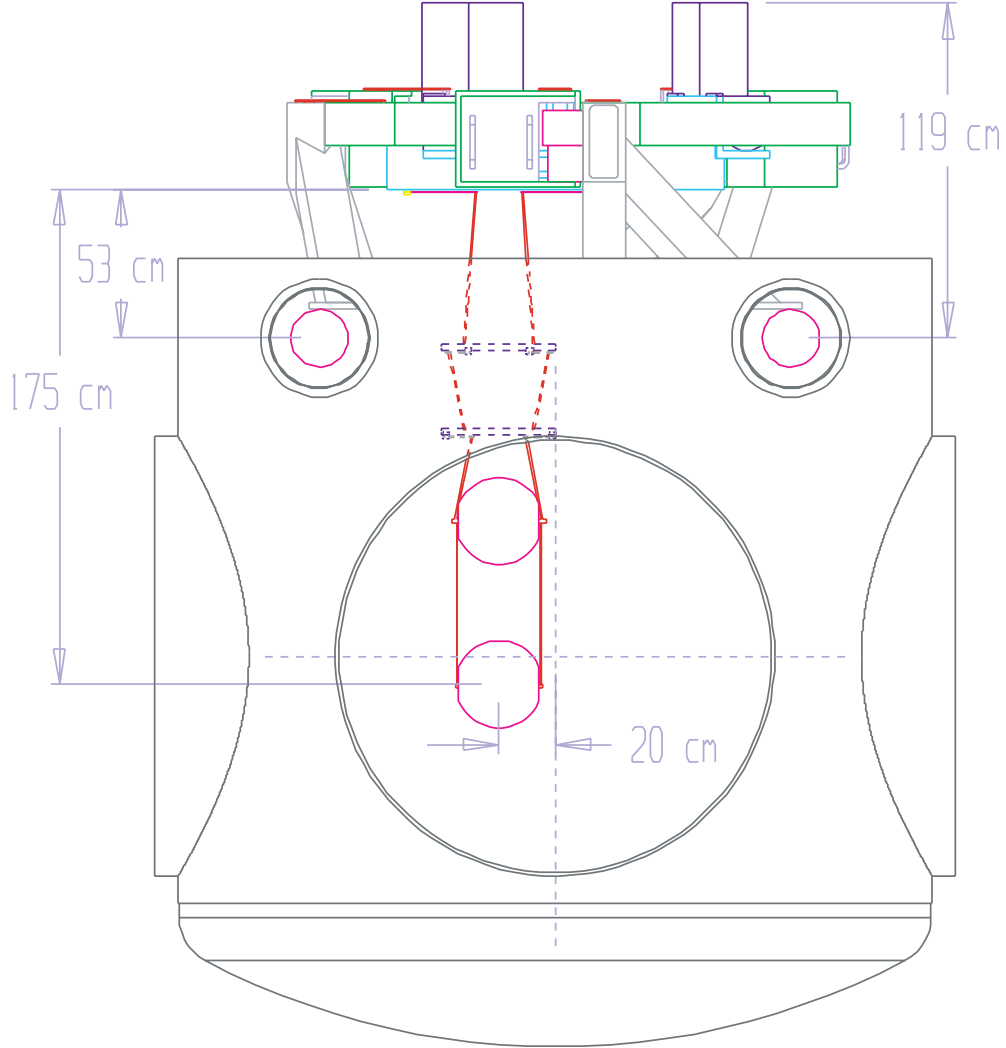
Figure 2: Elevation drawing of the baseline BSC chamber design. The GEO quadruple pendulum is shown to scale, with its required beam position when mounted on the two-stage active isolation platform's optics table. The external hydraulic actuators are not shown here.

replaced with a **quiet hydraulic actuator** that can move the in-vacuum SEI components by ± 1 mm with a bandwidth of 2 Hz in all six degrees of freedom. This should allow higher performance feed-forward correction of low-frequency ground noise and sufficient dynamic range for Earth tides and thermal or seasonal drifts. We expect approximately a factor of 10 reduction of the microseismic ($3 \times 10^{-2} - 3 \times 10^{-1}$ Hz) motion, from feedforward correction in this stage. For corrections up to the full ± 5 mm at each bellows, large screw adjustments are included in series with each hydraulic actuator.

The LIGO-I seismic isolation stack will be replaced with a **two-stage active seismic isolation platform.** As introduced above, vibration in each of the two cascaded stages is reduced by sensing its motion in 6 DOF's and applying forces in feedback loops to reduce the sensed motion. The outer stage derives its feedback signal by blending three real sensors for each DOF—a long-period broadband seismometer, a short-period geophone, and a relative
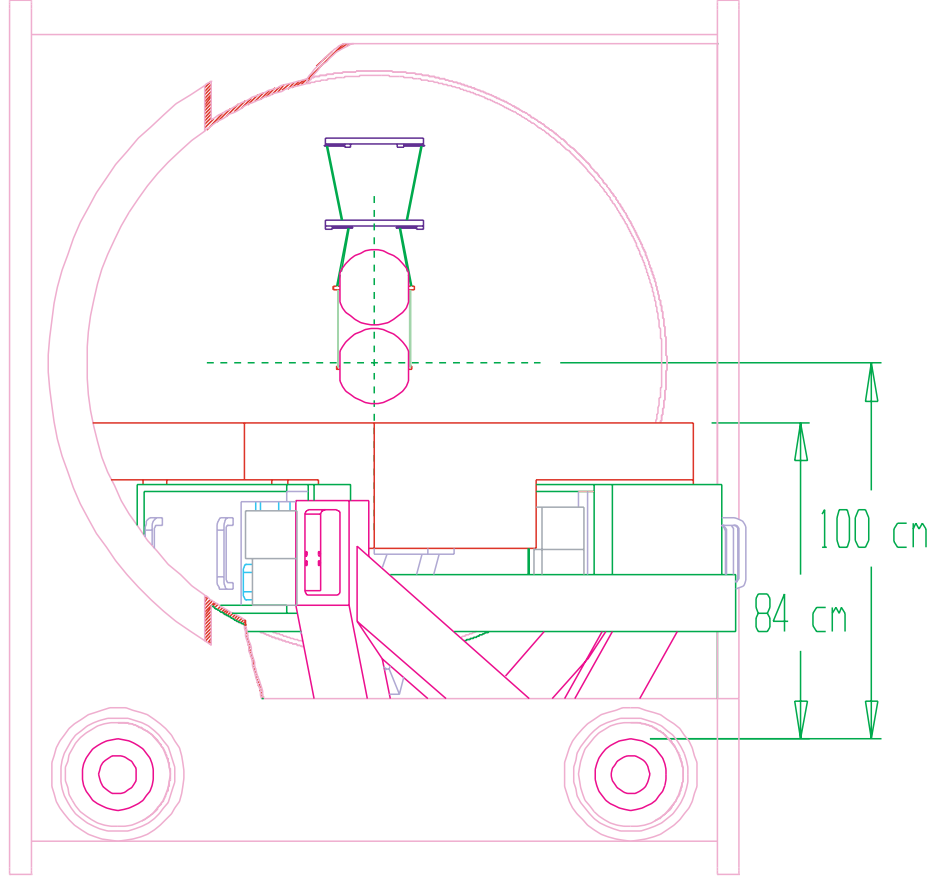
Figure 3: Elevation (cut-away) drawing of the baseline HAM chamber design. The dashed lines indicate beam center for a typical suspension position. The external hydraulic actuators are not shown here.

position sensor. The inner stage lacks the long-period seismometer, so has less feedback gain at low frequencies, including the microseismic frequencies. However, the low noise floor of the outer stage seismometer allows feedforward correction to the inner stage, and we expect an additional factor of 10 reduction in that range. Performance is described in greater detail in 3.

2 Design Description

2.1 Hydraulic external actuation

Conventional hydraulic actuators are found in many high force positioning applications. The conventional approach is not applicable here because of the high frequency fluid noise generated at all internal orifices. The field of quiet hydraulics is based on maintaining laminar flow throughout a system so as to eliminate high-frequency noise caused by turbulence. Our decision is to use a quiet hydraulic external actuator to continuously control large displacements of the SEI payload via control reallocation from the more sensitive loops, and
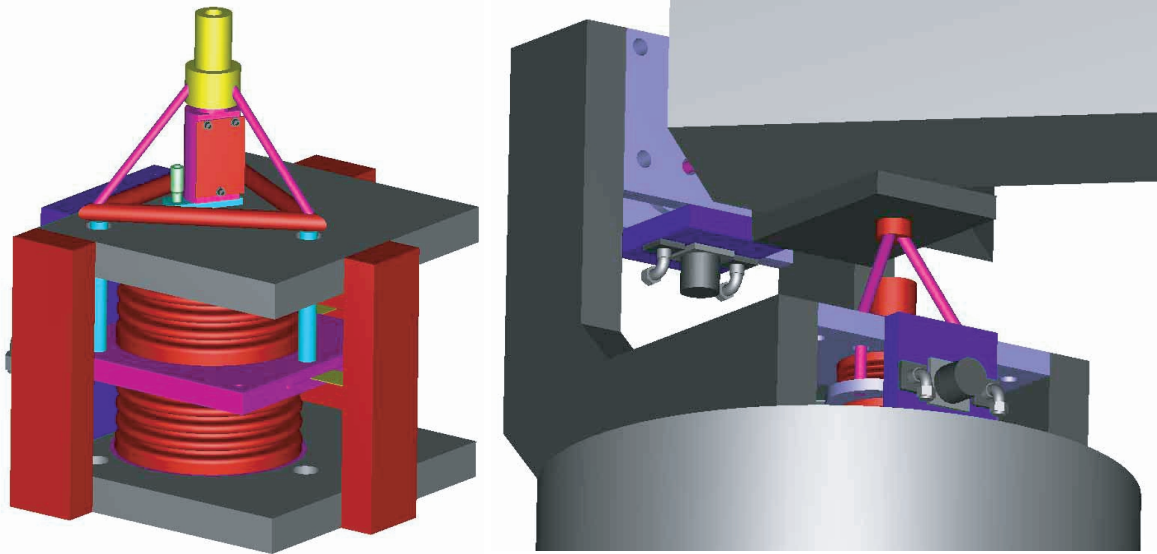
Figure 4: The Quiet Hydraulic Actuator. The gray blocks and red pillars form the reaction frame and are fixed in place. The two red bellows are pumped differentially to move the center purple actuation plate. The yellow bolt at the top attaches to the payload, and the actuation plate is attached to the payload by the rod assembly. An optical sensor (red and magenta) is placed between the yellow actuation point and the frame to allow low frequency servo stabilization. The figure at right shows two single-DOF actuators in place at the top of a SEI pier.

via feedforward based on signals from floor-mounted long-period seismometers.

The bandwidth and range described above can be achieved with a fluid working pressure of 75 psi. The pump power requirements remain modest by virtue of the relatively low upper unity gain point at 2 Hz. Since the velocities involved are extremely small (on the order 100 μm/s) with vertical actuation of a 2000 kg mass, the power requirements are quite small: Power = force · velocity = m · g · v = 2000 kg · 9.8 m/s^2 · 10^{-4} m/s = 2 W for the combined vertical actuators. Only a few tens of watts of pumping power are needed per chamber, and we plan to put the pump away from the LVEA/VEA slab. The quiet hydraulic actuator (Figure 4) is mechanically similar to a standard hydraulic piston. However, in order to avoid the stiction and leakage associated with conventional pistons, bellows are used as actuation cavities. The system runs with a viscous working fluid, mineral oil, and is engineered to maintain laminar flow while ensuring the hydraulic resonances are kept above 40 Hz. Figure 5 describes the continuous-laminar-flow differential-actuation scheme.

The displacement will be held against a hydraulic stiffness associated with a natural frequency of about 10 Hz. The hydraulic actuator we are developing will have an impedance that changes from being dominated by its support spring to being dominated by the viscous resistance at about 0.1 Hz. Thus, the velocity if accidently released at full stroke will be less that 1 mm/s. It will return to its rest position with a smooth exponential decay.
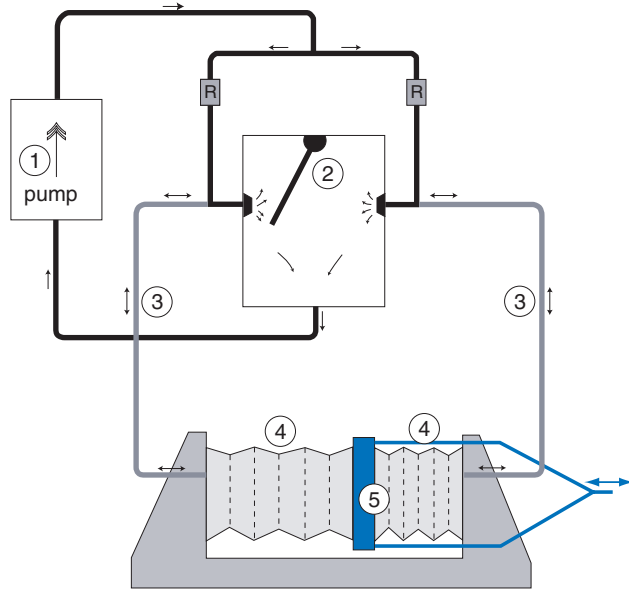
1. Viscous hydraulic fluid is pumped continuously into the control valve from 2 sides, and fluid is returned from a common point.

2. The control valve can move between the two inlets, creating a pressure differential on the different sides of the valve. The hydraulic resistance of the input lines (R) is balanced, so this system becomes the hydraulic equivalent of a Wheatstone bridge.

3. Tubing connects the two sides of the valve to the two sides of the differential bellows.

4. The differential bellows move when the pressure on the two sides is different.

5. The middle plate is attached in with flexures to both the base and the payload. The actuation point is constrained to apply force in one dimension, but is soft in all other degrees of freedom.

6. An optical displacement sensor (not shown), whose the output is corrected for seismic motion by a long-period seismometer, is placed between the moving block and the frame for servo stabilization.

Figure 5: Flow diagram of a single quiet hydraulic actuator.

2.2   Two-stage active isolation platform

Figures 6 and 7 show the BSC and HAM configurations of the cascaded two-stage active isolation platform. The stages are suspended through stiff blade springs and short pendulum links, giving natural frequencies in the 2 - 4 Hz range. This high suspension frequency means that the system's expansion sensitivity to temperature is about what you would expect from solid metal of the same linear dimension; the response of softer systems is often dominated by the change in the vertical suspension spring constant (through the temperature dependance on the spring material's Young's modulus). The inner plaform stage is built around a 1.5 m diameter optics table (BSC) or a larger rectangular table (HAM). For each suspended optic, the SUS is mounted on this flat table, and may be positioned and oriented as desired.
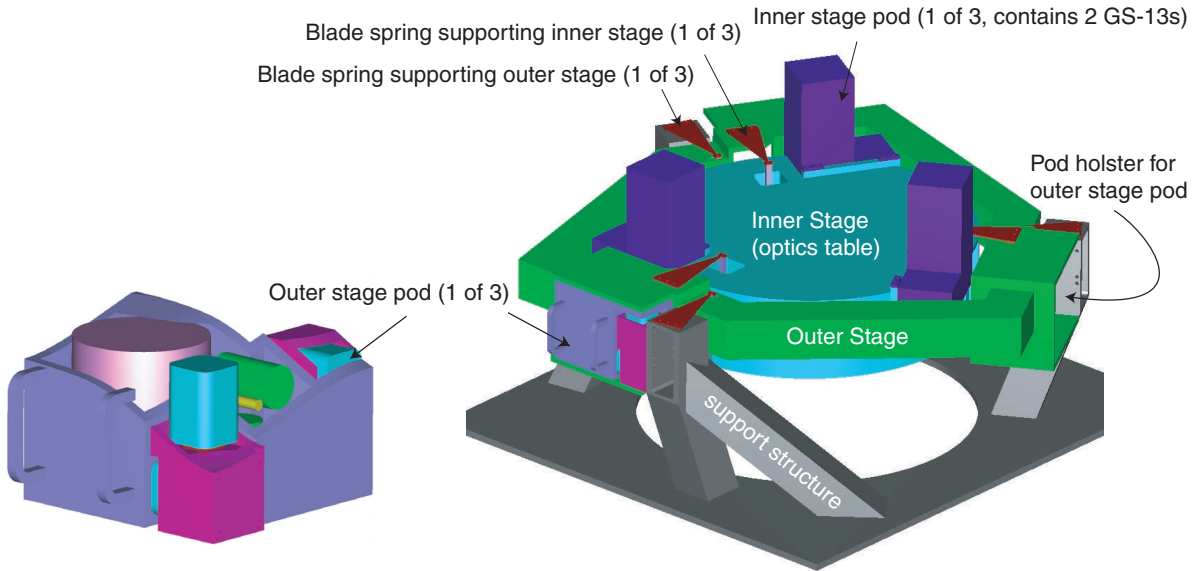
Figure 6: Rendering of BSC design of the two-stage active platform, shown without the surrounding BSC. The blue inner stage is built around the optics table interface that supports the suspension pendulums that hang down through the hole shown in the gray SEI support table. The height shown is correct for the current SUS design. The inset at left shows one of the field-removable instrumentation pods, common to both platform configurations, that houses the STS-2 long-period seismometer (pink), actuator magnet and coil (blue), and small geophones (green). The only instruments outside this pod, the large GS-13 geophones, are shown in purple and are mounted directly on the inner stage.

Local damping and noise-reduction control signals are generated for each DOF using a blended signal derived from short- and long-period seismometers and relative position sensors, which are described in section 2.2.1. The actuators are electromagnetic non-contacting forcers, which apply forces between adjacent stages, and are also described in 2.2.1.

The two-stage active seismic isolation platform resembles the pre-prototype built and tested at JILA over the past decade [6]. However, it has been refined and extended based on ideas and experimental work carried out at Stanford. The JILA development effort was directed towards a different goal (to detect GWs at 1 Hz), so our design has benefited from the JILA experience and 3-D modelling effort without the need for the ultra-high-performance seismometers that were part of JILA's development work (and an impediment to robust operation). Instead, we will use commercial, off-the-shelf seismometers, greatly simplifying the scheme and reducing risk. The choice of stiffer suspension also promises better thermal drift performance. The JILA experience, plus Stanford work (see, for example, [7]) on optimal sensor blending, feedforward techniques, the benefits of stiff suspension, and the practical use of modern control methods have led to our reference design. The less flexible JILA dynamic model has now been retired in favor of that described below (section 3) and in [3] and [2].
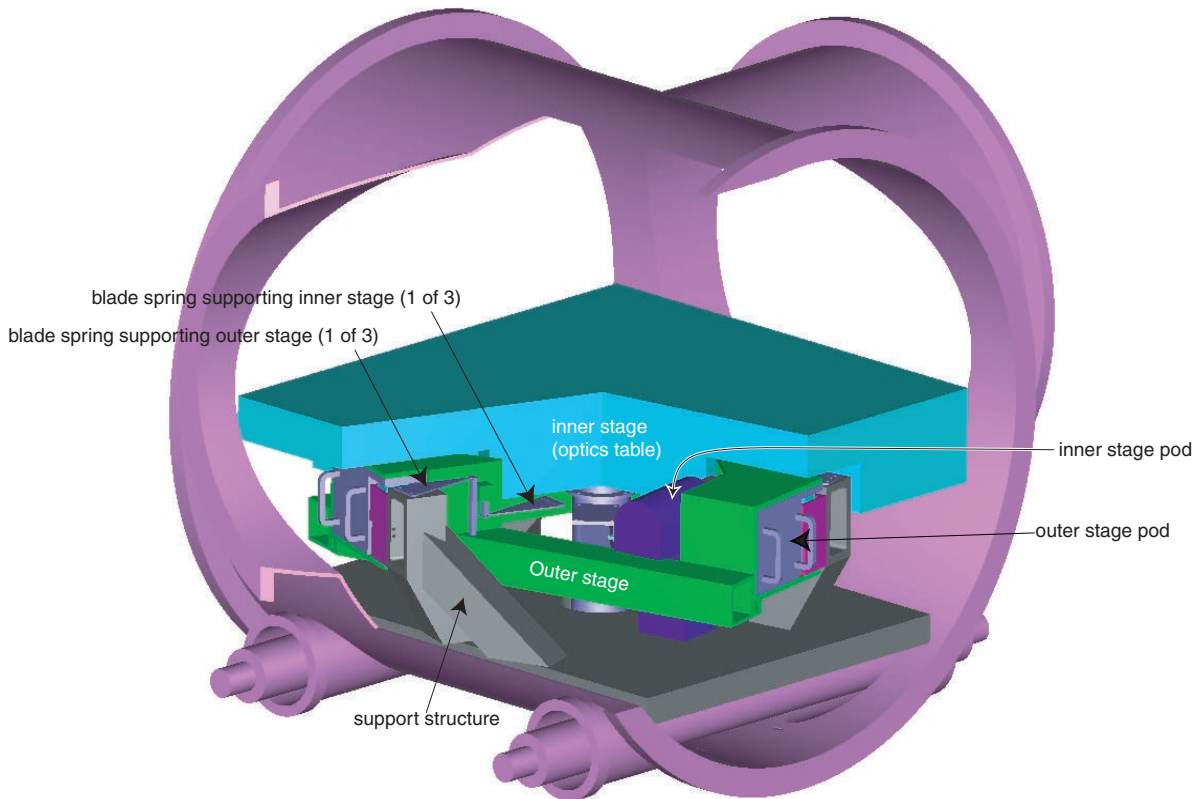
Figure 7: Rendering of the HAM design. Note that the instrumentation pods are positioned so that they are removable through the large HAM doors. The inner stage optics table (blue) is the same size as the table in LIGO-I, and in the same position.

One of the primary design goals of the pod was to keep the sensors and actuators of each stage as collocated as possible. It is well known that this collocation greatly robustifies the control design for flexible systems [10]. This design requirement resulted in the tight pod packing shown in Figure 6, but the benefits of this approach, in terms of simplifying the control design, are clearly shown in Figure 15.

2.2.1 Sensors and actuators

We have identified a set of sensors and actuators, described below, that are appropriate for the LIGO-II isolation system. We are currently testing all but the capacitive displacement sensors in our two prototype experiments, further described in [4]. Parts of these sensors will need to be encapsulated in small chambers filled with trace gas, complete with electrical feedthroughs; this is accomplished largely by confining them to the pod drawer. Some parts, such as the "target" side of the capacitive sensor and the bare metal target for the proximity sensor, don't require encapsulation. The equivalent displacement noise levels for these sensors are shown in Fig. 8.
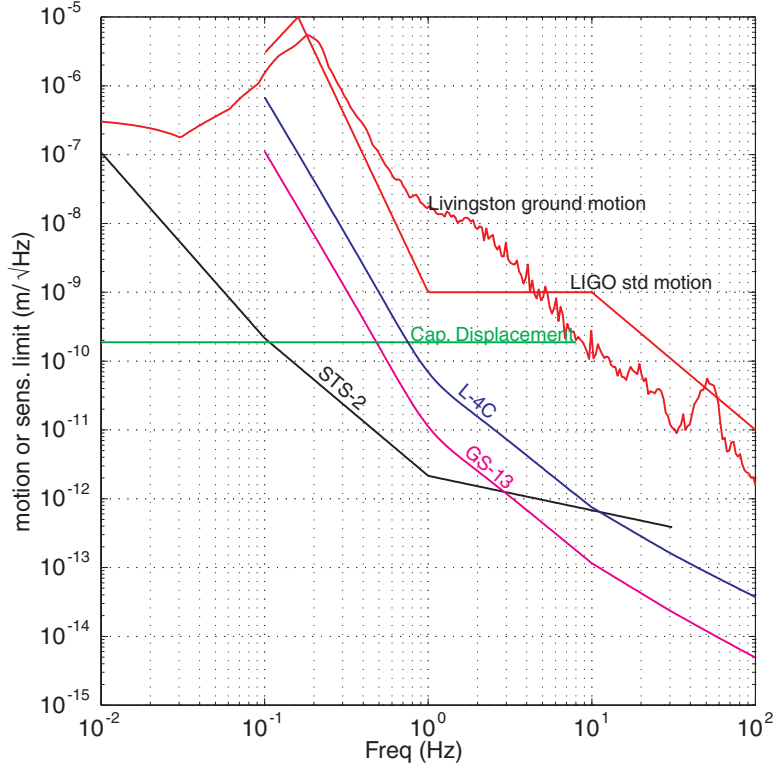
Figure 8: Displacement noise in various sensors used in the two-stage active isolation platform, compared with the LIGO standard ground noise and the measured noise at LLO. Note that the STS-2 can resolve motion approximately 5 orders of magnitude below the ground noise at microseismic frequencies.

Proximity sensor: The relative position sensor used in the stiff team's double active stage prototype is an inductive proximity sensor, model Bi5-M18-LIU made by Turck Inc. This is a non-contacting sensor that requires only a flat piece of metal as a target. The sensor package is a threaded cylinder 18 mm in diameter by 60 mm long; it is mounted with its end 3 mm from the target. The sensor has a linear range of 2 mm and an equivalent displacement noise of about 10^{-7} m/$\sqrt{\text{Hz}}$ at 0.01 Hz. Mounting, alignment, and operation are all very easy. The sensor may be operated in vacuum, though some modification will be necessary to make it suitable for use in a UHV system.

Capacitive bridge sensor: The inductive proximity sensor is sufficiently quiet for use in the LIGO-II active platform outer stage, and can even be used in the inner stage by using aggressive blending filters between it and the GS-13 short-period seismometer. However, to simplify the filter design and improve robustness, we intend to use another off-the-shelf sensor, the Queensgate NXD NanoSensor, which has a 1.25 mm range and a noise level of 1.8×10^{-10} m/$\sqrt{\text{Hz}}$. This Queensgate sensor's form is a thin 2 cm by 2 cm square, and it measures displacement with respect to a similarly sized metal plate using a capacitance bridge. This sensor is available in a vacuum compatible version.

10
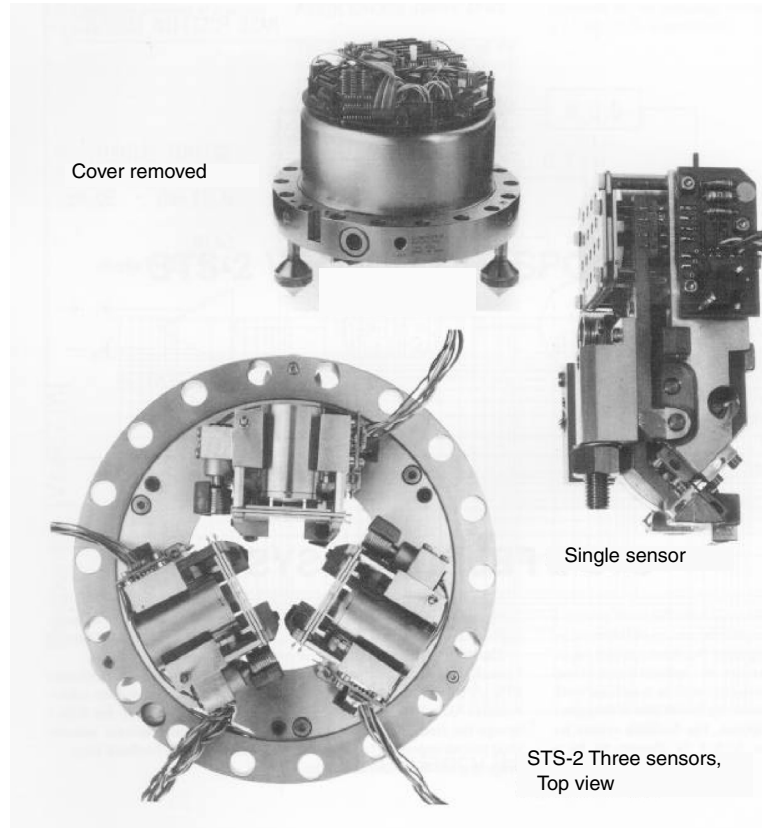
Figure 9: A broadband long-period vibration sensor usable from tens of millihertz to tens of hertz. Each STS-2 seismometer, manufactured by Streckeisen AG, measures vibration in three degrees of freedom. A vacuum-tight domed cover is included but not illustrated here.

Streckeisen STS-2: Figure 9 shows the STS-2 seismometer manufactured by Streckeisen AG. It is the standard for low-noise, very broadband seismological measurements. The casing is a cylinder 23.5 cm in diameter and 26 cm tall, and it houses three identical proof masses, arranged symmetrically about a vertical axis. Each proof mass is held in the center of its range by a servo using capacitive sensing and coil/magnet actuation; the servo error signal is a measurement of the ground motion. The signals from the three proof masses are electronically combined to give two orthogonal horizontal outputs and one vertical output. The response of the servo is tailored to give an approximately flat velocity response from 20 mHz to 50 Hz. In this frequency regime, the linear range of the seismometer is enormous, around 26 mm/s. The noise floor can be seen in Figure 8; it is several orders of magnitude below typical seismic noise at 0.1 Hz. There are no internal mechanical resonances below 100 Hz. The STS-2 may be operated in vacuum (as we intend to do in the double active stage prototype); however we anticipate enclosing it in a sealed case for the LIGO-II application.

Geophone: The GS-13 seismometer manufactured by Geotech Instruments LLC is a low-noise geophone. Its package is identical to that of the widely used (over 5000 units in the field) S-13 seismometer made by the same company: a cylinder 17 cm in diameter and 38 cm

from base to handle. It is convertible between horizontal and vertical operation, and has a natural frequency adjustable between 0.75 and 1.1 Hz. The noise floor is shown in Fig. 8. The seismometer is designed to be submersible and may be operated in vacuum, though for use in LIGO we anticipate housing it in a separate sealed enclosure with a preamplifier. Each unit has a mass of 10 kg.

Magnetic actuators: Our prototype experiments have used non-contacting voice coil and permanent magnet forcers, some homemade and some made by BEI Kimco. There are two kinds, a round voicecoil dipping into a radial magnetic field, and a set of opposing rectangular coils moving in a quadrupole field. Both types are available off-the-shelf, though the round design is offered in a greater variety of sizes and with larger magnet gaps (and therefore actuation range), so has been chosen for our current prototype tests, and calculations indicate that the round design will not compromise the prototype performance. The quadrupole magnet design offers reduced sensitivity to stray fields and reduced emission, as well as less cross-coupling of force between the stroke and transverse axes. For this reason, we plan to procure custom-made forcers based on the quadrupole design for LIGO-II, so we can have the desired large gaps in an interference-resistant configuration.

3   Performance model

We have used our new modeling tools [2] to make a preliminary prediction of the performance of the double active stage within the vacuum system. These results show that a double layer active platform should be able to achieve an isolation of 5×10^3 at 10 Hz, using a mix of both active and passive isolation. This is comparable performance to that demonstrated in the JILA platform, at 1 Hz [6]. We also achieve significantly more reduction of the RMS noise, since (unlike the JILA system) the reference design has active loop gain in the microseismic region. Each of the two stages is 200 kg, and is suspended by blade springs. The motions of the stages are modeled in all DOF (a total of $6 \times 2 = 12$). We have fitted the stages with an array of sensors and actuators, and the control is accomplished with twelve single-input single-output (SISO) loops. This model is therefore conservative, not taking into account any benefits the may be obtained with multi-input multi-output techniques and feed-forward. The preliminary modeling of the test mass motion is done in two steps (Fig. 10). First, the ground motion and sensor noise is used as an input to the model of the stiff double-active stage, and the motion of the inner stage is computed. The inner stage is the optics table, and is the suspension point for the pendulums. The inner stage motion is then used as an input to the GEO pendulum models supplied with [5].

Although these are preliminary results, they should accurately represent the performance of the two-layer active platform, without feedforward; they are summarized in Table 1. We have also estimated the additional benefit of feedforward low-frequency noise reduction from the ground noise to the hydraulic stage and between the two active in-vacuum stages. We summarize the total performance that includes these estimates in parentheses in Table 1 (page 16).
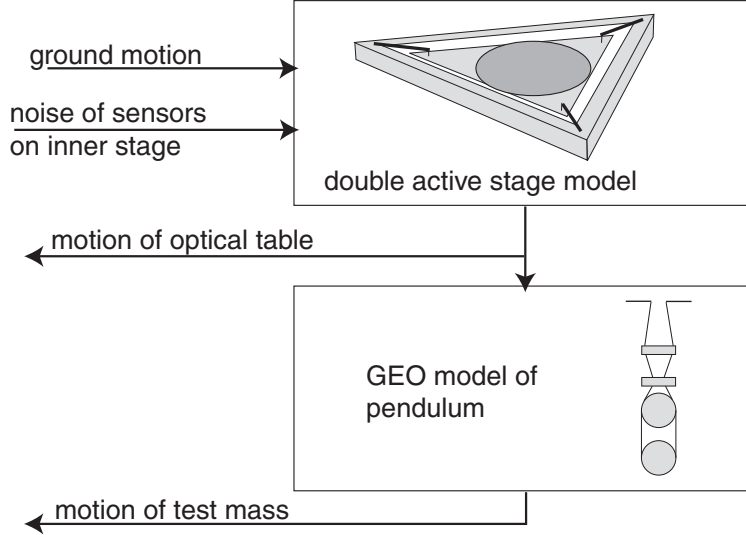
Figure 10: The Model results were generated in a two step process. First, the motion of the optical table was simulated using sensor noise and ground motion. The motion of the optical table was then used as an input to the GEO pendulum model to compute test mass motion.

3.1   Preliminary model particulars

Arrangement of the sensors: The sensors and actuators are placed on the stages at the actual design positions so that they sense the real dynamics of the platforms at the sensed position, not the idealized translations at the mass center. This means the model can properly simulate the coupling of the various rigid-body modes of the plant into the sensors and actuators.

Relative position sensors: The low frequency sensors we use are relative displacement sensors (e.g., we use the Queensgate NXD NanoSensor in the noise models of the inner active stage). Relative position sensors improve the stability of the system by eliminating low frequency cross-overs in the servo compensation loops. However, since they are relative position sensors, they effectively lock the stages together over the frequency range where they provide the dominant loop gain, short-circuiting the isolation of the system. In order to properly model the performance of such a system, one must distinguish between relative motions of the isolation stages and absolute motion of the stages in inertial space. The model takes the position sensor signals as the distance, along the vector orientation of the sensor, between sensed points on each platform. As a result, the isolation predictions (see, for example, Fig. 12) correctly indicate that there is no isolation at low frequencies, even though there is high loop gain.

Sensor Noise: The noise from the sensors is one of the basic limits on the performance of the active isolation system. We have modeled the sensor noise for the critical components of the model, the sensors on the inner active stage. The noise models of the sensors are shown in Fig. 8.

Relative Actuators: The model includes the back reaction effects of the forcers which act on the inner active stage. These act by pushing against the outer active stage. The back reaction causes coupling between the inner and outer stage loops, so it must be included to properly model the plant dynamics.

3.2 Preliminary model results summary

We feel the preliminary results are quite reasonable, since they capture the important dynamics of the system: the mechanical cross couplings of the stages in 6 DOF, the readouts of relative sensors between 2 moving stages, and the back-reaction forces of actuators between two moving stages. The model predicts a motion of the test mass in the beam direction of 1×10^{-20} m/$\sqrt{\text{Hz}}$ at 10 Hz, when the local controls of the quadruple pendulum are off. If the quad pendulum controls are left on, and noise in the pendulums local control sensors is ignored, we predict a test mass motion of 1×10^{-19} m/$\sqrt{\text{Hz}}$ at 10 Hz; both cases meet the LIGO-II requirement.
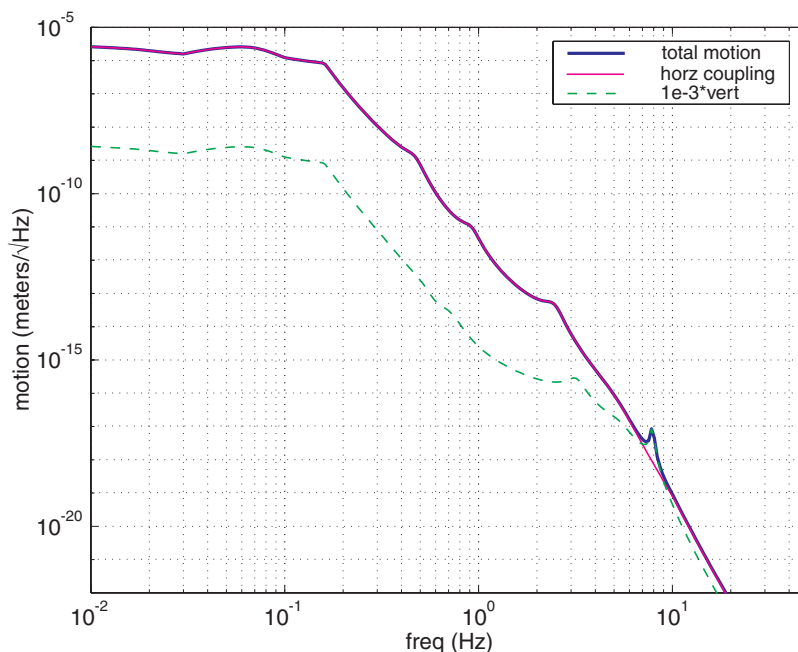
Figure 11: Motion the test mass (ITM and ETM), assuming local pendulum damping loops are on, but noise-free. If the local pendulum controls are turned off, the noise at 10 Hz is reduced by an additional factor of 10, because the ground noise coupling is reduced. This curve does not reflect the additional noise reduction of feedforward in the two-stage active platform and the hydraulic stage.

Generation of the Test Mass Motion: These calculations were done by simulating the motion of the inner stage of the isolation system (the optics table) in the vertical and horizontal directions, and multiplying motion by the transfer functions generated by the GEO
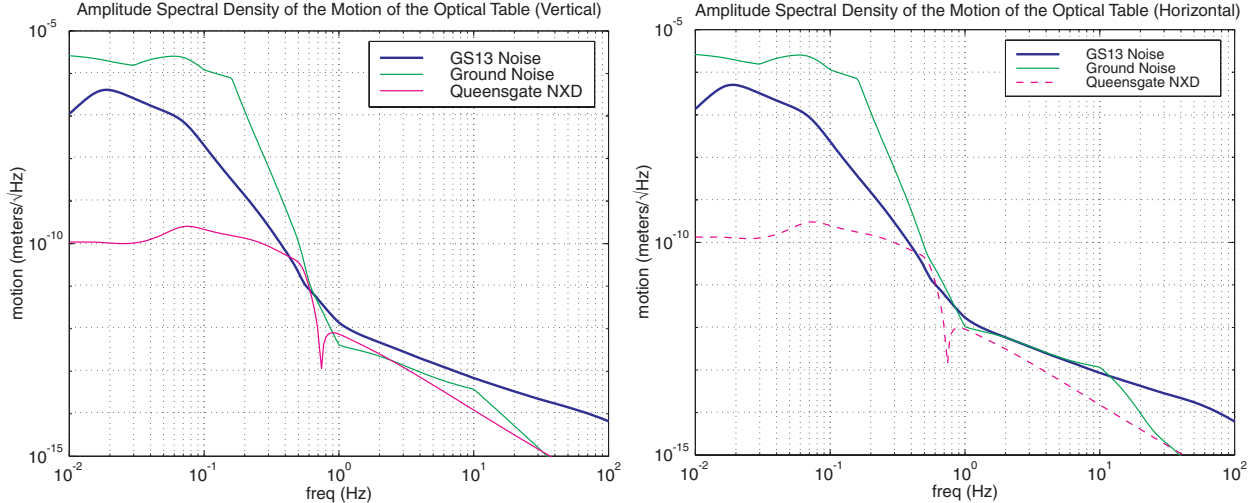
Figure 12: Performance of the two-stage active platform, without feedforward. Here we plot the contributions to the noise level at the SEI optics table, the suspension system mounting point.

Matlab routines from reference [8], `mc_reference.m` and `qp_reference.m`. The horizontal and vertical motion of the optics table is generated by independently simulating the amplitude response of the table to ground motion given by the LIGO Standard Spectrum, the noise of the GS-13 geophone, and the noise of the Queensgate NXD NanoSensor.

The 10 Hz noise of the mode cleaner optics in the HAM chambers is predicted to be 1×10^{-18} m/$\sqrt{\text{Hz}}$ when the pendulum local control is turned off, and 5×10^{-18} m/$\sqrt{\text{Hz}}$ with the local control on.

The stiff system significantly improves the RMS performance of the pendulums. There are two RMS numbers which are of interest. The first is the RMS velocity of the test mass while the interferometer is unlocked, which is needed for lock acquisition calculations. The second is the RMS position of the test mass while the interferometer is locked, which is used to calculate various noise couplings to the GW signal. We use the GEO model of the global controller to determine the RMS motion of the test mass while the interferometer is locked. Using the 200 Hz upper unity gain frequency, we calculate the RMS motion of the mirror under global control assuming the pendulums suspension point motion is the optical table motion. The RMS velocity of the test mass is computed by calculating the velocity of the test mass without global control, assuming the suspension point motion is given by the motion of the optical table.

When we add the isolation of the external stage, the RMS position and velocity numbers will both improve by approximately a factor of 10, since they are both dominated by the microseismic motion. We therefore meet the major requirements, using only a preliminary model of the two-stage platform. As the model improves, we will be better able to improve the low frequency performance, and study the modifications which are necessary to make the control laws appropriate for the system with its the final mass and sensor distributions, and compensate for the integrated pendulums.

The model of the stiff double-active-stage system can be thought of as a series of functional blocks, illustrated by the Simulink diagram we used to run the model. The model

15

	units	optics table	BSC test mass	HAM test mass
$x(f)$ at 10 Hz	m/$\sqrt{\text{Hz}}$	2×10^{-13}	1.0×10^{-20} [1×10^{-19}]	2×10^{-18} [3×10^{-18}]
RMS displacement	m	6×10^{-7} (1×10^{-8})	4×10^{-17} [1×10^{-14}]	
RMS velocity	m/s	3×10^{-7} (3×10^{-9})	4×10^{-17} [1×10^{-9}]	

Table 1: Key noise levels calculated for the reference design, *without (with) the beneficial effects of the hydraulic stage and feedforward.* Test mass RMS noise is calculated by integrating the spectral density down to 0.01 Hz, with the global length control loops on. Only 5×10^{-12} N RMS global control force is needed at the test mass actuator when the SUS is mounted on the active platform, compared with 1×10^{-8} if mounted on the ground. Blank fields have not yet been calculated, but are expected to be within requirements. [requirements] are shown bracketed in red.

includes several parts:

1. a set of test inputs and outputs.

2. a mechanical model of the two stage system.

3. a set of sensors which are distributed on the outer stage.

4. filters which blend the outer stage sensors into six super-sensors.

5. a set of sensors which are distributed on the inner stage

6. filters which blend the inner stage sensors into six super-sensors.

7. a set of actuators between the outer stage and the ground.

8. a set of actuators between the inner stage and the outer stage.

9. a set of 12 SISO control laws which connect the 12 actuators with the 12 super-sensors.

A typical loop is one of the vertical controllers on the inner stage (stage 2 in Fig. 13). There are two sensors to consider for this loop, the Queensgate relative position sensor, and the GS-13 1 Hz geophone, an inertial instrument. The signals from these two sensors are blended together as shown in Fig. 14.

3.2.1   Operating modes

The SEI system has five operating modes, normal operation, normal without global control input, a high-damping mode for protection and safety during periods extremely high motion, a mode for SEI lock acquisition, and a diagnostics/calibration mode.
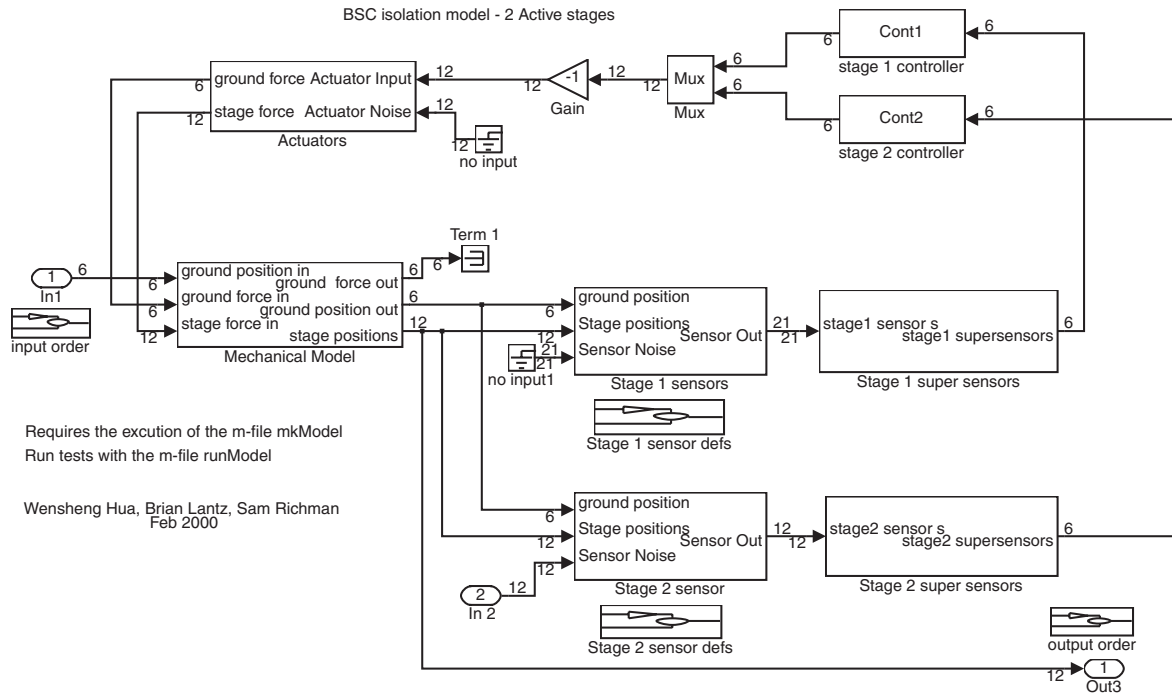
Figure 13: Simulink model used to calculate the dynamics and servo compensation in the reference design two-stage active platform. Such a design is then used to cross-compile the controller using the dSpace DSP hardware, as is being done in the current prototype experiments. The controllers represented by the blocks Cont1 and Cont2 do not have any coupling between the loops. There is loop interaction because of the nature of the relative position sensors, the actuators, and the mechanical couplings in the double platform. However, by collocating the sensors and actuators, the system is easily controlled with a diagonal compensator (SISO loops).

Normal operation: Global control signals generated by the ISC interferometers are feed back to the various stages in the SUS. As SUS control signals depart from their quiescent values, control authority is reallocated to the SEI, first to the active platform and finally to the fine hydraulic actuators external to the vacuum system. The goal in designing this reallocation it to keep most sensors and actuators at the center of their range as drifts due to thermal effects and Earth tides change lengths and alignments. Also, as in LIGO-I, ground seismometer signals are used to generate a feedforward signal intended to cancel the microseismic motion, and this is applied to the fine actuators. For the "normal operation" mode, the SEI servo compensation is optimized for routine low-noise detector operation.

Normal without global control: During some periods of detector operation is may be necessary to operate the SEI without any global control reallocation, even at extremely low frequencies, and instead take up all of the angle and length drift in the SUS. For this mode, the local position sensors will control the DC position. The capacitive displacement sensors have an RMS position error of order nanometer, so the total position drift in this configuration will likely be limited only by thermal expansion coefficients of the (preexisting)
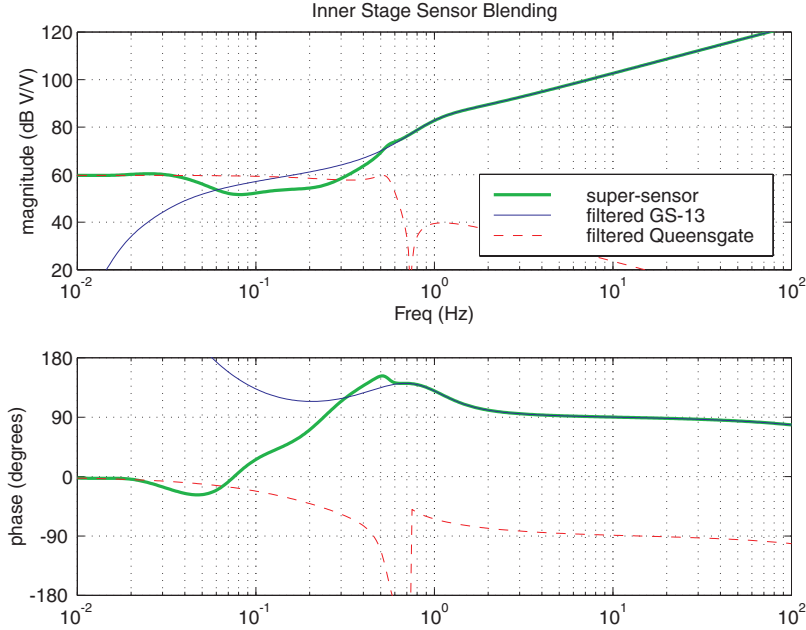
Figure 14: Blending of the inner stage vertical sensors. Aggressive filtering of the sensors occurs once the sensor is no longer the dominant signal source of the loop. This is done to improve the performance of the systems. Additional thought must be given to the blending filters to insure they are robust to reasonable changes in the gain of the sensors. Once the sensors have been combined, they can be thought of as a single, broadband sensor which we call a "super-sensor." The control can then be designed between the 12 actuator inputs to the isolation system, and the 12 super-sensors. The outer stage loops have two blend frequencies (not shown), to combine three sensors into one super-sensor.

external SEI components and the LVEA/VEA slab. As does the previous mode, this mode still allows low-noise detector operation.

This mode might also be used during ISC lock acquisition.

High-damping, minimum impulse response: During periods of exceptionally large environmental noise, such as during installation when the vacuum system is open, or during earthquakes, the system can be switched to a mode where its impulse response is minimized and the servo loops are not destabilized when mechanical range limits are reached. A fail-save test in the operating code can be programmed to switch the power off if even this mode results in unacceptable motion, thus relying on the hard mechanical limits to limit system damage.

SEI acquire lock This is the mode that systematically closes the active servo loops of the SEI two-stage active platform.

SEI diagnostics and calibration This mode will be used periodically to calibrate the sensors and actuators, and to measure the "plant" properties; this includes "system identification."
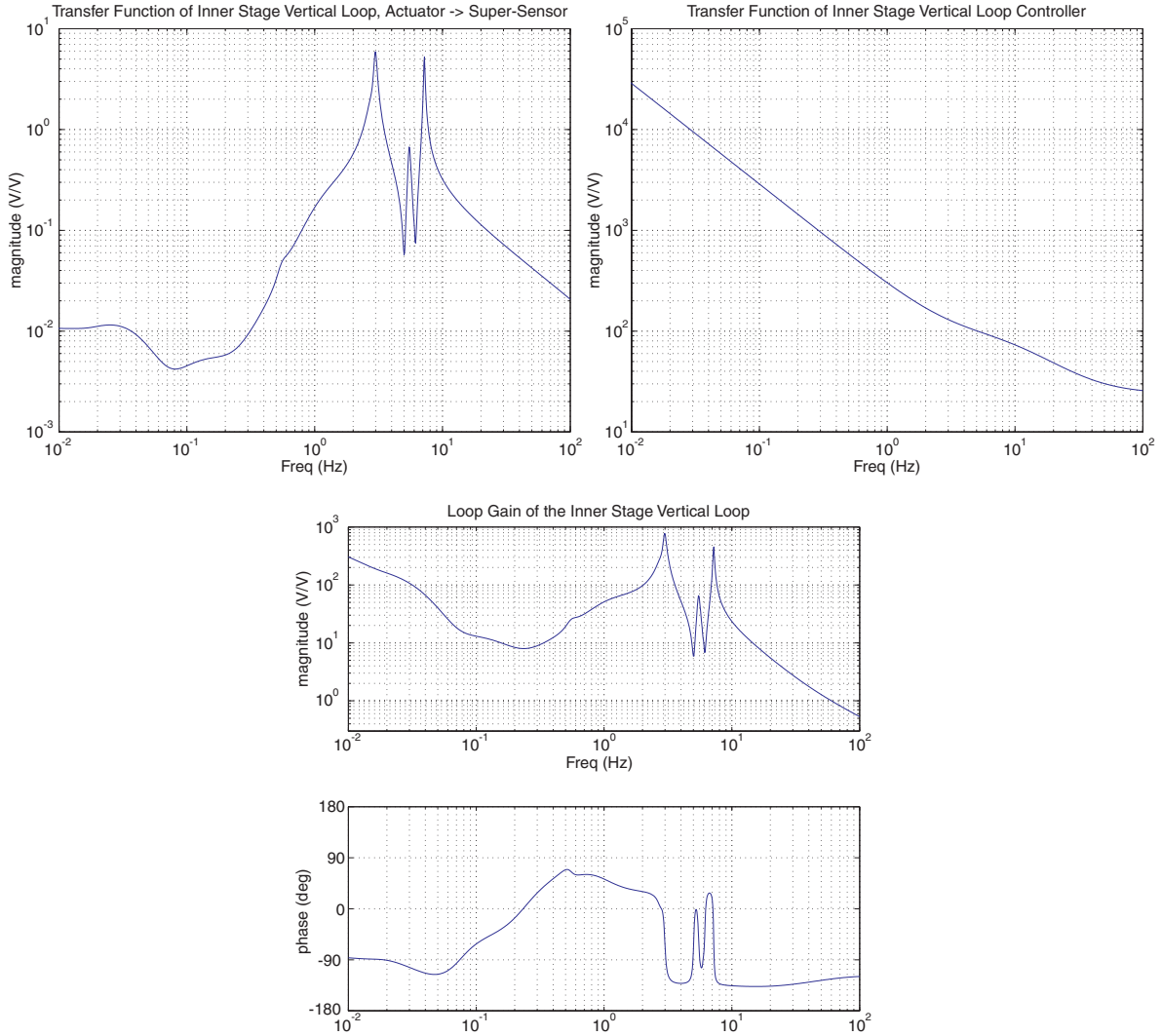
Figure 15: *upper left:* Transfer function from inner stage vertical actuator #1 to its collocated super-sensor. The input and output units are both volts. This system is quite well behaved, so designing a SISO controller is quite simple. *upper right:* A simple system based on an integrator was chosen as the control law. *lower:* This results in a system with an open loop gain which varies between 10 and 30, excluding mechanical resonances. The mechanical resonances are quite large, but are well controlled when all the loops are closed, so the system has only one cross-over, and that upper unity gain frequency is between 60 and 70 Hz, depending on which of the twelve loops you consider.

3.3 Other requirements

Vacuum compatibility: The structural elements in the two-stage active platform will be made of the same materials with the same methods as were used to make the LIGO-I SEI optics tables and downtube, so we expect there to be no problems with vacuum compatibility in these elements.

The seismometers will be enclosed in sealed chambers within the pods (except for the

inner stage GS-13, which has its own enclosure), filled with trace gas to allow leak testing. The STS-2 dissipates approximately 2 W of heat in normal operation; this can easily be removed via copper ribbons, since the dynamics of the "stiff" suspension will be unaffected by reasonable wiring and heat conductors.

The coarse (inductive proximity) position sensors have a working distance of several mm from the metal face, so if necessary the face can be enclosed behind a thin glass window and the rest encapsulated. The fine (capacitive bridge) sensors are available commercially prepared for vacuum use from Queensgate.

The magnet/ voice coil actuators can be prepared for vacuum use, by winding the coils with Kapton-insulated wire.

Cabling accommodation: Wiring for the inside the vacuum envelope can be exactly as used in LIGO-I. The large number of channels should not be a concern as long as they are routed to prevent rubbing, since the suspension will be much stiffer than the wires. There are obvious surfaces for wire routing (see Figs. 6 and 7).

Earthquake resistance: Figs. 6 and 7 also illustrate the heavy stage frames, which highly constrain the motion of the stages with respect on one another. Heavy stop screws will be adjusted to prevent the voice coils in the actuators from ever touching the magnets. In minor earthquakes, the active isolation system and hydraulic stage are switched to a high-damping mode to limit test mass suspension shaking, even when physical stage-to-stage contact is made.

Diagnostic information: Since every rigid-body degree of freedom is monitored, with a total of 30 measurement channels inside the vacuum system for each SEI, continuous monitoring of diagnostic information comes automatically. These channels can be made available on the reflected memory loop and archived as desired.

Also, as part of the occasional system identification routine necessary for feedforward noise reduction, all transfer functions are measured and can be observed over time for changes and checked against models.

References

[1] D. Shoemaker, D. Coyne, "LIGO-II Seismic Isolation Design Requirements Document." 11/4/1999. LIGO E990303-02-D

[2] Brian Lantz, Wensheng Hua, Sam Richman, Jonathan How, "Computer Modeling and Simulation in Support of the Stiff-Suspension Active Seismic Isolation for LIGO II," 2/14/2000, LIGO T000016-01

[3] Wensheng Hua, Brian Lantz, Sam Richman, "How to construct mechanical model of a mass-spring system," http://lsuligo.phys.lsu.edu/active/pen3.pdf

[4] B. Lantz, R. Stebbins, C. Hardham, J. Giaime, "The experimental program in support of stiff-suspension active seismic isolation for LIGO-II," 2/14/2000, LIGO T000015-00.

[5] "LIGO II Suspension: Reference Designs," by the GEO Suspension Team, (distributed within the LSC) 1/31/2000.

[6] Richman, S.J.; Giaime, J.A.; Newell, D.B.; Stebbins, R.T.; Bender, P.L.; Faller, J.E.; "Multi-stage active vibration isolation system," Review of Scientific Instruments, **69:6**, 2531. (June '98)

[7] Hong Sang Bae, "Active Vibration Isolation and Alignment Issues for LIGO," Masters Thesis, Department of Mechanical Engineering, Stanford University, August 1999.

[8] distributed by the GEO suspensions team in January, currently available at `http://www.ligo.caltech.edu/~dhs/l2_sus_ref1.tar`

[9] Peirce, S. Tran, H., Wiedemann, M., and DeBra, D., "Quiet Hydraulics for Ultraprecision Actuation," in Proceedings of ASPE Spring Topical Meeting on Mechanisms and Controls for Ultraprecision Motion, Tucson Az., 1994.

[10] Joshi, S. M., "Robustness Properties of Collocated Controllers for Flexible Spacecraft," AIAA Journal of guidance control and dynamics, **9,** number 1, 85–91. (1986)